



COVID-19 lockdowns drive decline in active fires in southeastern United States

Benjamin Poulter^{a,1}, Patrick H. Freeborn^b, W. Matt Jolly^b, and J. Morgan Varner^c

^aEarth Sciences Division, Biospheric Sciences Laboratory, NASA Goddard Space Flight Center, Greenbelt, MD 20771; ^bRocky Mountain Research Station, Fire Sciences Laboratory, US Forest Service, Missoula, MT 59803; and ^cTall Timbers Research Station, Tallahassee, FL 32312

Edited by Ruth DeFries, Columbia University, New York, NY, and approved August 17, 2021 (received for review April 6, 2021)

Fire is a common ecosystem process in forests and grasslands worldwide. Increasingly, ignitions are controlled by human activities either through suppression of wildfires or intentional ignition of prescribed fires. The southeastern United States leads the nation in prescribed fire, burning ca. 80% of the country's extent annually. The COVID-19 pandemic radically changed human behavior as workplaces implemented social-distancing guidelines and provided an opportunity to evaluate relationships between humans and fire as fire management plans were postponed or cancelled. Using active fire data from satellite-based observations, we found that in the southeastern United States, COVID-19 led to a 21% reduction in fire activity compared to the 2003 to 2019 average. The reduction was more pronounced for federally managed lands, up to 41% below average compared to the past 20 y (38% below average compared to the past decade). Declines in fire activity were partly affected by an unusually wet February before the COVID-19 shutdown began in mid-March 2020. Despite the wet spring, the predicted number of active fire detections was still lower than expected, confirming a COVID-19 signal on ignitions. In addition, prescribed fire management statistics reported by US federal agencies confirmed the satellite observations and showed that, following the wet February and before the mid-March COVID-19 shutdown, cumulative burned area was approaching record highs across the region. With fire return intervals in the southeastern United States as frequent as 1 to 2 y, COVID-19 fire impacts will contribute to an increasing backlog in necessary fire management activities, affecting biodiversity and future fire danger.

COVID-19 | fire | forest

In early 2020, policies were implemented worldwide to prevent and slow the spread of the coronavirus disease 2019 (COVID-19). These policies mandated the closure of workplaces, forcing a large proportion of society to “work from home,” starting first in Asia in February 2020 and then across North America in mid-March 2020. Almost immediately, as society adjusted in ways never experienced before, changes were observed in air quality (1), water quality (2), surface vibrations (3), and nightlights (4). For example, reductions in atmospheric nitrous oxide concentrations were measured over almost all urban centers and travel corridors across the globe (5). Improvements in water quality due to reduced turbidity from shipping activity revealed new inland-water habitats for fisheries (6). Annual carbon dioxide (CO₂) emissions declined between 5% and 7% for 2020 (7), detectable from energy consumption data (8) and also from the Orbiting Carbon Observatory-2 (OCO-2) greenhouse gas satellite (9), although surprisingly, the growth rate of atmospheric CO₂ remained the same as previous year (10). To help track the indirect and direct effects of COVID-19 on the Earth system, new frameworks proposing novel feedbacks have emerged (11, 12). Pathways highlighted in these frameworks suggest interacting impacts of COVID-19 on natural ecosystems via reductions in air pollution that would affect cloud condensation nuclei and mesoscale climate processes and that longer-term impacts of COVID-19

on CO₂ emission reductions would affect even longer-term climate dynamics (11).

Beyond weather and climate, however, human activities directly impact ecosystem structure, composition, and function through forest management, fuelwood harvest, and deforestation (13). In most parts of the world, fragmentation and habitat degradation have also affected disturbance processes, such as fire (14). Fire is a natural process and is found in almost all terrestrial ecosystems where fuel loads, moisture conditions, and ignition sources converge to support combustion and fire spread (15). Modern fire is an increasingly anthropogenic process, with fire suppression, ignitions, and fragmentation from land-cover change or drainage of peatlands creating novel fire regimes and increasing the need for active management, such as prescribed fire (16). In the United States, over 80% of wildfires are caused by a combination of intentional and unintentional human ignitions, accounting for more than 40% of annual burned area (17). Human-ignited prescribed fires typically exceed or mirror annual wildfire extents in the United States (18). Because of this relationship between humans and fire, consequences from COVID-19 would likely have direct impacts on ecosystems, rather than indirect, by affecting both the number of ignitions and the effectiveness of fire suppression. For example, by mid-March 2020, fire management activities on public and private lands in the United States were temporarily shut down as state and federal agencies closed or as fire managers postponed prescribed fire plans to reduce the

Significance

The coronavirus pandemic, COVID-19, led to strict social-distancing guidelines that severely impacted human livelihood and economic activity. Workplace closures reduced travel, and early in spring 2020, improvements in air and water quality, reduced seismic activity, and reductions in greenhouse gas emissions were observed. COVID-19-related shutdowns emerged at the beginning of the prescribed fire season in the southeastern United States, where 80% of fires are human caused. Using active fire satellite observations and fuel treatment statistics, we estimated a 21% reduction in active fires from March to December 2020 (up to 40% on federal lands). This reduction in active fire may increase fire risk in the future and is detrimental to biodiversity and other ecosystem services inherent to fire-dependent ecosystems.

Author contributions: B.P., P.H.F., W.M.J., and J.M.V. designed research; B.P., P.H.F., W.M.J., and J.M.V. performed research; B.P. and P.H.F. analyzed data; and B.P., P.H.F., W.M.J., and J.M.V. wrote the paper.

The authors declare no competing interest.

This article is a PNAS Direct Submission.

This open access article is distributed under [Creative Commons Attribution-NonCommercial-NoDerivatives License 4.0 \(CC BY-NC-ND\)](https://creativecommons.org/licenses/by-nc-nd/4.0/).

¹To whom correspondence may be addressed. Email: benjamin.poulter@nasa.gov.

This article contains supporting information online at <http://www.pnas.org/lookup/suppl/doi:10.1073/pnas.2105666118/-/DCSupplemental>.

Published October 18, 2021.

risk of transmitting COVID-19 in the workplace, exacerbating smoke-related respiratory problems to nearby communities, or as fire crew members were affected by contracting COVID-19 themselves. In addition, concerns about fire suppression capabilities were raised, for example, how to safely support emergency wildfire firefighting crews that typically live in close quarters and in large numbers (19, 20).

Here, we present results on how COVID-19 affected fires in the southeastern United States, a landscape of fire-dependent ecosystems categorized in the “intermediate-cool-small” pyrome (21). This pyrome is strongly influenced by human activities, both in natural and managed systems, including agriculture (22). Agricultural fires in the region account for about 16% of fire counts, with about 35% of fire counts in Florida attributed to agriculture (22). The forested ecosystems in this nine-state region,* covering 1.2 Mkm², include longleaf pine (*Pinus palustris*) savannas that support numerous threatened and endangered plant and animal species, given the requirement for fire to occur as frequently as 1 to 2 y (23). Using remote-sensing data from the NASA Land, Atmosphere Near real-time Capability for Earth Observing Systems Fire Information for Resource Management System (FIRMS), we were able to track fire activity at subdaily frequency and compare these observations to historical records from the past 20 y. Tracking active fires has relevance for informing fire managers, interpreting changes in air quality, and identifying increased fire danger risk from “missed” fuel treatments. An unusually wet spring, with cold fronts driving heavy precipitation events, required that meteorological effects be separated from how COVID-19 affected fire ignitions. Thus, we developed an empirical model to predict fire activity based on historical meteorological conditions and range of variability and evaluated the COVID-19 effect as the departure from this forecast. To substantiate uncertainties in the satellite record (e.g., downlink problems experienced with the Moderate Resolution Imaging Spectrometer [MODIS] aboard Aqua in late August and early September 2020), we also evaluated prescribed fire statistics reported for federally owned lands in the region managed by the US Departments of Agriculture (National Forests) and Interior (National Wildlife Refuges, National Parks, and Preserves).

Decline in 2020 Active Fires Detected from Space

The NASA FIRMS database provides near-real time (NRT) access to active fire data for a number of space-based satellite instruments. Here, we used two of the longer-term active fire datasets from 1) the MODIS instrument onboard the Terra (launched December 1999) and Aqua spacecraft (launched May 2002) and 2) from the Visible Infrared Imaging Radiometer Suite (VIIRS), launched October 2011, and one of several instruments onboard the Suomi National Polar-Orbiting Partnership. Using multiple instruments helps overcome limitations in overpass time (24), with the Local Time Descending Node for Terra at 1030 and 2230 hours, Aqua at 1330 and 0130 hours, and VIIRS at 1330 and 0130 hours. In addition, the instruments have different spatial resolutions at nadir (1 km for MODIS and 375 m for VIIRS) and sensitivities to surface temperature anomalies, which provides an opportunity to evaluate detection efficiency of small fires.

Almost immediately following the stay-at-home orders issued in mid-March 2020,[†] a drop in the number of active fire

detections across the southeastern United States was observed (Fig. 1A). The decline was even more pronounced on federally owned lands (Fig. 1B), which saw almost no fire from mid-March until October 2020 (week 40). Across the coastal plain from Alabama through Georgia, active fires were lower than the long-term mean (Fig. 1C), and by April, the declines over federal lands were visually striking across the landscape (Fig. 1D). Relative to 2003 to 2019, the decline in annual active fire by state (SI Appendix, Fig. S2) was largest for the states of South Carolina (37%), Tennessee (33%), and Mississippi (28%). On federally owned lands (SI Appendix, Fig. S3), Georgia had the largest decline (68%), followed by Tennessee (57%) and South Carolina (51%). By the end of 2020, active fires were 21% lower than average relative to MODIS era, 2003 to 2019 (third lowest), and 10% lower relative to the VIIRS era, 2012 to 2019 (second lowest). On federally owned lands, the reduction in active fires was 41% for MODIS and 38% for VIIRS, the lowest recorded for both eras.

Between early February and mid-March, cold fronts brought substantial precipitation across the southeastern United States (SI Appendix, Fig. S5) at the same time when prescribed fire activity typically peaks (25, 26). By mid-February, cumulative precipitation (SI Appendix, Figs. S6 and S7) was higher than observed since 1980 for the states of Arkansas, Alabama, Mississippi, Louisiana, Tennessee, and South and North Carolina but remained low for Florida. Negative active fire anomalies were observed for all states and ownerships in this time period between early February and early March (Fig. 2A and B), but it is possible smaller fires did not decline as much as detected by VIIRS (Fig. 2C and D). In the last week of February and first 2 wk of March 2020, active fire anomalies were observed to be close to average or positive across almost all states and ownerships (Fig. 2A–D), bringing the number of active fire pixels back to average counts for this time of year (SI Appendix, Figs. S2 and S3). After March 15, 2020, however, fire activity abruptly declined following the stay-at-home orders, continuing the decline until late June, when private landowners then took advantage of opportunities to burn in summer (e.g., mid-July to August; Fig. 2A and C). In contrast, on federal lands, the active fire pixel counts remained anomalously low until late November and early December when fire activity increased again in Arkansas, Louisiana, Mississippi, and Alabama (Fig. 2A and C).

Decline in Prescribed Fire from Statistical Reporting

Remote sensing of active fires does not discriminate between wildfires, prescribed fires, and the burning of biomass on agricultural lands (22). Additionally, remote sensing of active fires is an imperfect record of thermal anomalies when clouds are present, when fire sizes or intensities are imperceptible, or when fires are burning between overpasses. To confirm the satellite record, we used statistics on prescribed fire burn area utilized for fuel treatments reported by US federal land management agencies within the Department of Agriculture (i.e., US Forest Service) and the Department of Interior (i.e., the Bureau of Land Management, US Fish and Wildlife Service, National Park Service, and Bureau of Indian Affairs). The data reported by the Department of Agriculture to the Forest Service Activity Tracking System database and the data reported by the Department of Interior to the National Fire Plan Operations and Reporting System database are integrated by the National Wildfire Coordinating Group to develop a harmonized Integrated Interagency Fuels Treatment Decision Support System (IIFTDSS) (27).

Similar temporal trajectories were observed in the satellite-based active fire data and the interagency fuels treatment data (SI Appendix, Fig. S4) using IIFTDSS prescribed fire categories

*The study area includes the states of Mississippi (125,434 km²), Louisiana (134,264 km²), Alabama (135,765 km²), Arkansas (137,732 km²), Florida (170,304 km²), Georgia (153,909 km²), South Carolina (82,932 km²), North Carolina (139,389 km²), and Tennessee (109,151 km²).

[†]The stay-at-home orders were advised at the federal level on March 16, 2020, and implemented at the state level for Mississippi (April 4), Louisiana (March 30), Alabama (April 3), Arkansas (none), Florida (April 3), Georgia (April 3), South Carolina (April 7), North Carolina (March 30), and Tennessee (April 2).

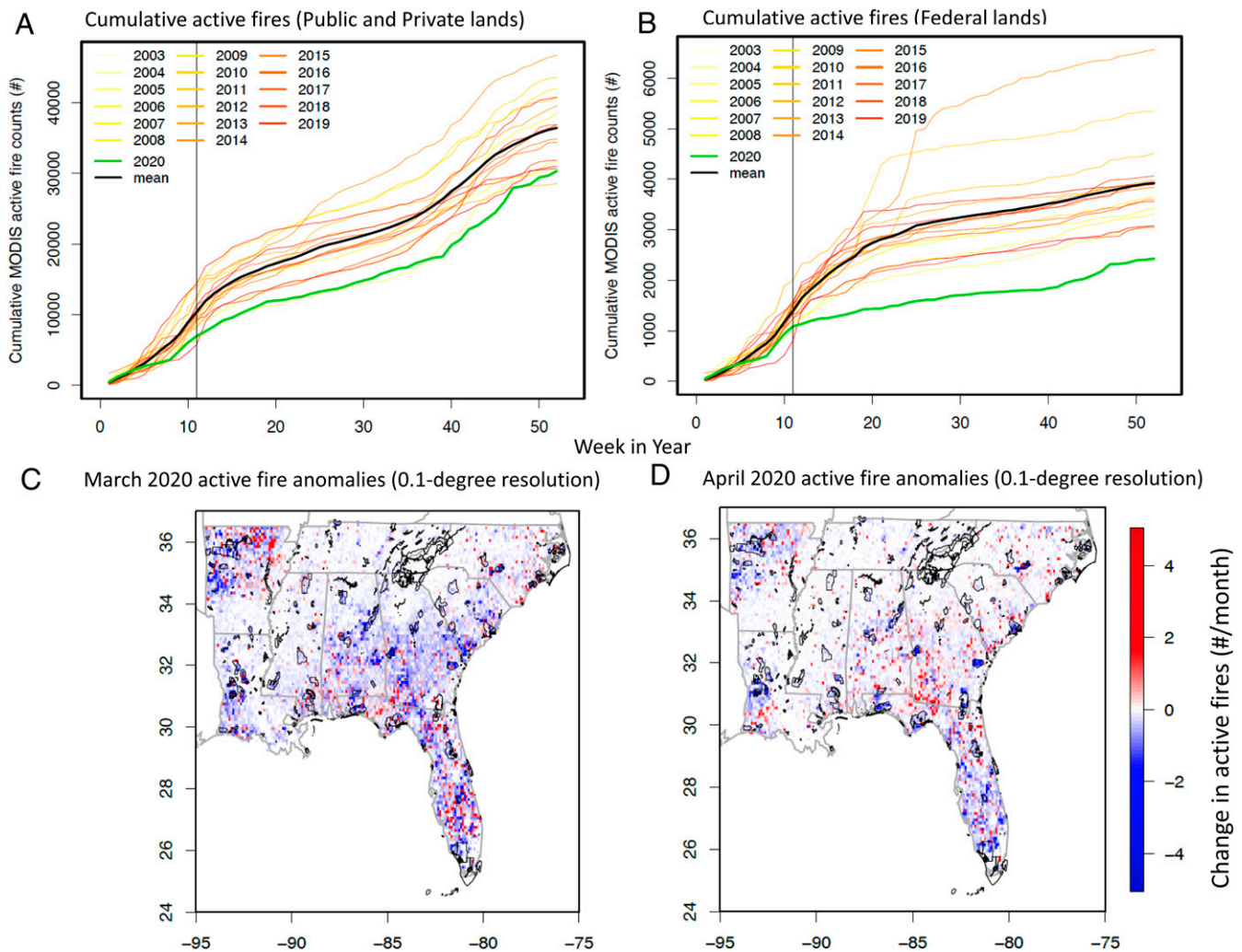


Fig. 1. Time series of cumulative active fire pixels detected by MODIS Aqua and Terra on (A) all lands and (B) federally owned lands (Department of Interior, Department of Defense, Department of Agriculture). The black vertical line in A and B is March 15, 2020, the approximate date of COVID-19-driven stay-at-home orders. Maps of (C) March 2020 and (D) April 2020 active fire anomalies (relative to 2003 to 2019) with federally owned lands shown by black polygons. See *SI Appendix, Fig. S1* for the same figures but using VIIRS (2012 to 2019).

(see *Materials and Methods*). Across the southeastern United States, the IIFDSS data showed a decrease in burned area during the high-precipitation period of February 2020 and then a rapid early March increase in burned area to levels greater

than on record. For example, by March 15, 2020, 2,050 km² of prescribed fire area was reported, relative to the previous 9 y average when only ~1,600 km² (minimum to maximum: 1,060 to 2,097 km²) was burned by this date. This was followed by an

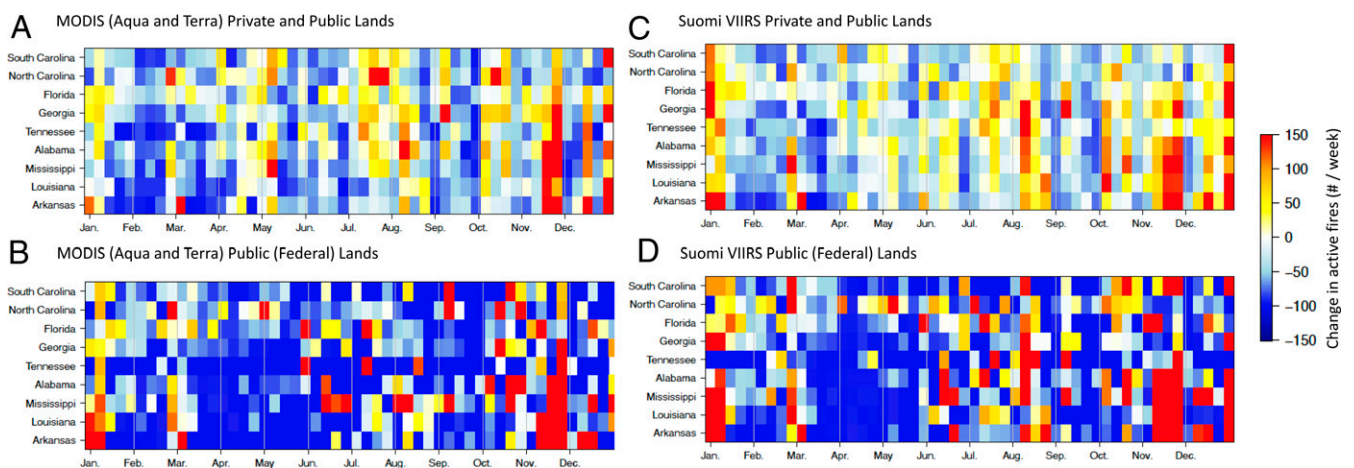


Fig. 2. Weekly active fire anomalies for the MODIS instrument in (A) all lands and (B) federal lands only and for the Suomi VIIRS instrument in (C) all lands and (D) federal lands only. The active fire anomalies are relative to 2003 to 2019 for MODIS and 2012 to 2019 for VIIRS.

almost complete cessation of prescribed fire in all states on March 15, 2020, when the federal stay-at-home orders were issued. At the end of 2020, just 2,850 km² of land was reported to have been burned during prescribed fire fuel treatments compared to the previous 9-y average of 3,480 km² (minimum to maximum: 2,865 to 4,333 km²), about a 21% reduction in burned area.

Meteorological Effects on Fire Danger

A statistical model was developed to forecast expected fire activity for March to August (MAMJJA) based on the Keetch-Byram Drought Index (KBDI) (28). We calculated KBDI using meteorological data from the NASA Global Modeling and Assimilation Office (GMAO) and used KBDI anomalies, relative to their 99th percentile, to fit a linear model (see *Materials and Methods*; see *SI Appendix, Table S1* for statistical summaries). Models were fit to MODIS Terra and Aqua active fire pixel counts for each state, both inside and outside federally owned lands. The MAMJJA period was chosen because it reflected the main period of COVID-19 social-distancing restrictions.

In all cases, the 2020 active fire pixel counts were significantly lower than what would have been predicted based on historical relationships for MAMJJA (Fig. 3). This departure from expected conditions illustrates the COVID-19 effect on fire activity and was stronger for federally owned lands. For example, active fires were as much as 42% (1-sigma range; 29.9% to 55.7%) lower than forecast on federal lands for Arkansas, 56% (21.2% to 90.8%) for Georgia, and 46.5% (24.9% to 67.9%) for Tennessee. While the model provided additional insight into the COVID-19 effect, the relationship is very much a first-order approximation of climate-fire behavior. More information to improve the statistical forecast at sub-state levels, including covariates for fire history, vegetation type, and fuel load, would contribute to reducing uncertainties.

Impacts on Trace Gas Emissions and Air Quality

Air quality was an early indicator that COVID-19 was affecting the Earth system due to changes in human behavior. Landscape fires are a source of particulate matter (PM_{2.5}) and other trace gases, and a reduction in their number would cause a decrease in emissions production. We used data from the Global Fire Emissions Database (GFED) and the Quick Fire Emissions Database (QFED) to evaluate whether the decline in active fires in 2020 led to a decline in carbon emissions. In 2018, fossil fuel consumption in the southeastern United States emitted 320 Tg C (Tg = teragram; 10¹² g). In comparison, wildfires in the southeastern United States emit between 11.7 and 23.9 Tg C y⁻¹ (1997 to 2020 average, 15.7 Tg C y⁻¹) based on QFED and 2.1 and 9.9 Tg C y⁻¹ (average, 5.7 Tg C y⁻¹) based on GFED. In 2020, fire emissions were the lowest on record (Fig. 4), with QFED reporting 11.9 Tg C y⁻¹ and GFED reporting 4.3 Tg C y⁻¹. While locally these reductions would be expected to affect air quality, at regional scales, the emissions represent less than ~3.7% of fossil fuel emissions and thus are unlikely to be detected as anomalies in atmospheric column observations of carbon monoxide or CO₂ (29).

Implications for Fire Management and Ecosystems

This study shows that COVID-19 had direct impacts on ecosystems by changing human behavior linked to fire management and ignitions. The reductions in active fires, prescribed fire area, and emissions production are the largest in the more than 20-y record (1997 to 2020). In contrast to the Western United States, where the 2020 fire season broke new records for area burned (17,000 km² burned in California alone), the southeastern United States had a very different fire year.

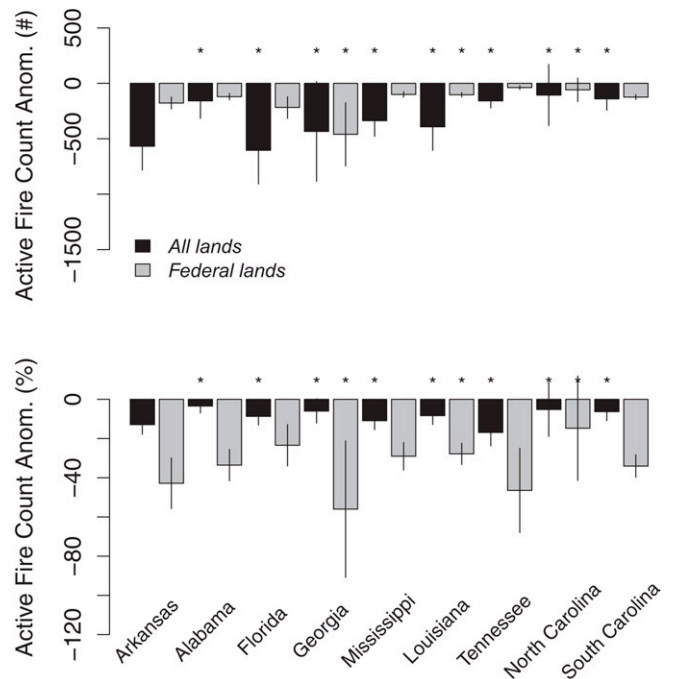


Fig. 3. Departure between expected MODIS active fire pixel detections based on the relationship with March through August mean KBDI for 2003 to 2019 and observed MODIS active fire pixel detections in 2020. Both the number of active fire pixel counts (*Top*) and the percentage relative to the average (*Bottom*) were lower than what would have been expected because of the COVID-19 effect on ignitions. The statistical model was consistent for federally owned lands, which showed significant decreases in fire relative to what was predicted. Error bars are 1 SD, and asterisks indicate the regression was significant at $P < 0.15$; for state-by-state summary, see *SI Appendix, Table S1*.

The consequences of reduced fire activity range from impacts on local and regional air quality (30) to direct impacts on biodiversity (31, 32) to impacts on fuel loading (33). Fire management in the southeastern United States is limited by seasonal burn windows and minimal resources (23), where large numbers of fires are needed to maintain short fire return intervals (1 to 3 y). Many rare and imperiled plant and animal species require frequent fire for the maintenance and recovery efforts (34, 35). Furthermore, the consequences of delayed or “missed” prescribed fires as effective fuel treatments may lead to more difficult fire suppression in the near term. Continually missed opportunities for burning contribute to accumulating backlogs. For example, 2019 was also a low burn year because of the US Government federal shutdown, or furlough, that lasted from December 22, 2018, to January 25, 2019 [the beginning of the peak period in annual burning (25, 26)]. Early data for 2021 show slightly above-average active fires, suggesting that fire managers are working through these backlogs when conditions permit.[‡]

Previous work shows that in the southeastern United States, fire-prone ecosystems with high productivity are associated with rapid recovery of living and dead fuels. In pine flatwoods, for example, significant differences in fuel loading, fireline intensity, and rates of spread result from just a single year of additional growth (36). Even in more xeric upland pine ecosystems, where productivity is lower, threshold responses occur in fuel load and corresponding ecological conditions affecting fire (37). These effects cascade to invertebrate and vertebrate

[‡]<https://talitimers.org/nasa-prescribed-fire-covid19/>

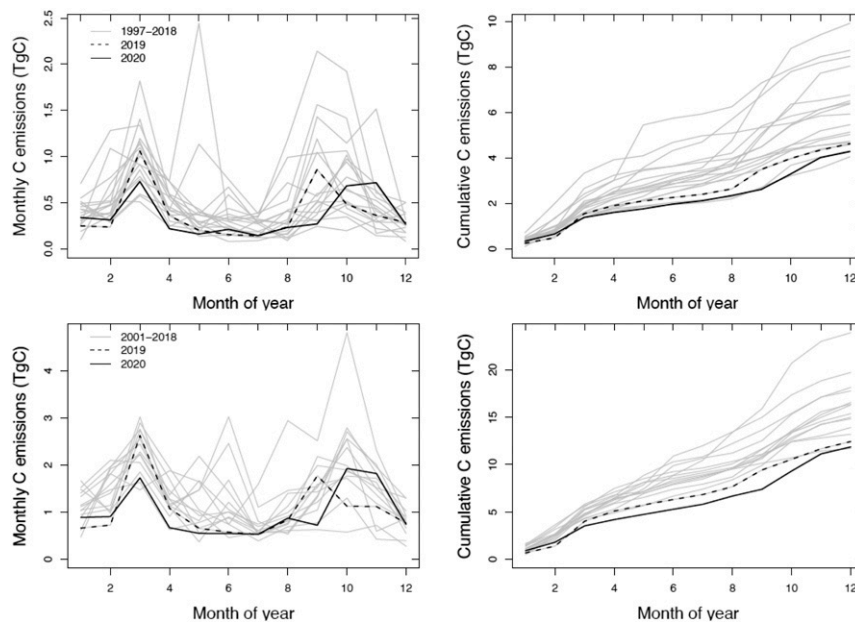


Fig. 4. Monthly and cumulative fire carbon emissions over the southeastern United States. The GFED (*Top*) and QFED (*Lower*) both showed that 2020 carbon emissions were lowest on record (as far back as 1997). This would also directly influence other trace gas emissions including CO_2 , CO, and CH_4 .

responses that can also be degraded with additional fire-free years in these frequent fire ecosystems (35). Based on the evidence from these long-term studies (37), potential continued COVID-19 restrictions lingering into the 2021 fire year may increase fire hazard and alter a variety of ecological conditions.

Combining remote-sensing observations with federal statistics helped address several limitations in the remote-sensing data. The remote-sensing uncertainties include time of day of overpass and obscuration of the land surface by clouds in spring 2020 but also errors of omission, as fire sizes may have become smaller as fire managers adapted to smaller fire crews. However, according to the IIFDSS data, median fire size for 2011 to 2019 was 1.5 km^2 and 2020 was 1.7 km^2 , but the data are not yet available for private lands. Private land permit data would also help reconcile uncertainties on nonfederal lands, but permit data often include area statistics for places that may not have actually burned if weather or plans changed after the permit was released (25, 34). Using multiple lines of evidence from diverse remote-sensing data combined with federal and state statistics offers a robust approach to characterize the spatial and temporal variation in fire.

To help managers prioritize upcoming burns, seasonal forecasts can help inform how the burn window is emerging under the changing climate (38). Fire danger has increased over the past decades (39), making prescribed fire more urgent but also more complex to implement (34, 40). The COVID-19 pandemic reveals how significantly humans have altered and controlled fires across the southeastern United States and elsewhere [i.e., smaller declines in Europe (41) and increases in Colombia (42)] and emphasizes the need for a combination of spaceborne and ground-based monitoring approaches to help inform and optimize fire management in the future.

Materials and Methods

Satellite Data. The active fire detections for the three sets of observations follow the same algorithm developed by refs. 43 and 44. This algorithm estimates land-surface temperature (LST) derived from thermal band emissivities in 4.0 μm for MODIS and 3.74 μm for VIIRS using Planck's blackbody function. For MODIS, we used day and night detections provided by the MCD14DLv006 product that combines Collection 6 Terra (MOD14) and Aqua (MYD14) fire products that use Collection 6 L1B MOD021KM and MYD021KM radiance

products. For VIIRS, we used day and night detections provided by the VNP14IMGTDL_NRT L2 VIIRS product that uses channel I-4 brightness temperatures for hot spot detection. The LST data are filtered for cloud effects, and then a set of threshold criteria are applied to determine whether the temperature anomaly is an active fire. No "confidence" criteria were applied to filter potential false positives in the active fire; instead, all active fire observations were used. The decision to include all active fire detections avoided introducing uncertainty into the application-specific criteria confidence value used (45). Including all confidence levels also allowed a more objective treatment of the active fire detections across all years and states to avoid biases in cases where fire size or intensity may change year to year. The data are available through NASA FIRMS at <https://firms.modaps.eosdis.nasa.gov/>, and a visualizer has been developed by Tall Timbers at <https://talltimbers.org/nasa-prescribed-fire-covid19/>.

Trace gas emission data were provided by GFED (GFED4.1S) and QFED (QFEDv2.5r1). The two emissions databases use different approaches to estimate burned area, with GFED4.1s using MODIS burned area (MOD45) and an internal carbon cycle model (46), whereas QFEDv2.5r1 (47) uses fire radiative power using the cloud correction method developed in the Global Fire Assimilation System from MOD14 and MYD14. Thus, a comparison between the two helps to quantify uncertainties and robustness of observations.

Ancillary Data. The US state boundaries were masked using the US Census Bureau state shapefile, `cb_2018_us_state_5m`, at a scale of 1:5,000,000. Federal ownership data were from the US Geological Survey Sciencebase Catalog, shapefile `fedlanp010g.shp_nt00966`, 1:1,000,000 scale. An error in the California Federal Information Processing System codes in `fedlanp010g.shp_nt00966` was corrected in which three properties incorrectly assigned California lands to Arkansas.

Federal fire management statistics for 2011 onward were downloaded on February 6, 2021, from the ArcGIS Online Integrated Interagency Fuels Treatments feature service.⁸ Fuel treatment types that incorporated prescribed fire included broadcast burns, hand pile burns, machine pile burns, and jackpot burns. Wildfires and wildland fire use fires that inadvertently burned a treatment plot or were used opportunistically as a fuel treatment were not included since these were likely unplanned events (*SI Appendix, Fig. S4*). The statistics are geospatial, provided in shapefile format, and were summarized based on the reported completion date.

Meteorology Data. Meteorological data from the NASA GMAO Modern-Era Retrospective analysis for Research and Applications, Version 2 (MERRA-2) Reanalysis were used to analyze precipitation trends and to compute the fire

⁸ <https://doitd.maps.arcgis.com/home/item.html?id=acdb4a650c824c91ba7efd51d3f9f008#overview>

danger index. MERRA-2 is an assimilation system that uses surface, aircraft, and spaceborne measurements to produce global, hourly, gridded meteorological variables (48). MERRA-2 data cover the time period of 1980 to present day at $0.5 \times 0.625^\circ$ spatial resolution. For this analysis, the variables T2MMAX (2-m air temperature) and PRECOTCORR [corrected precipitation (49)] were used. The variables were converted to daily mean temperature and daily total precipitation.

KBDI Calculation. The KBDI was developed in 1968 (28) as a simple fire danger index linking evaporative demand and precipitation to estimate cumulative moisture deficit representative of fuel. The KBDI was used partly because it was developed originally in the southeastern United States, but we acknowledge that a range of other fire danger indices, such as the Canadian Fire Weather Index, would be appropriate and yet give similar results at the spatial scale (state to region) that we investigate (50). We use MERRA-2 variables daily mean T2MMAX (TMAX, °C) and daily total PRECOTCORR (P, mm) as inputs for estimating KBDI. The KBDI values are transformed to their anomalies relative to 95th or 99th percentile values (described as follows).

We used standard set of parameters to estimate the soil moisture deficit, assuming a soil column (D) of 203.2-mm depth. Mean-annual rainfall (mm) was estimated for 2000 to 2019. The soil moisture deficit was initialized at 0 mm on day 1 of the simulation (and then applying Eqs. 1–6 on a daily time step), requiring less than a year to reach quasi-equilibrium (and last 21 of 41 y used in the analysis).

$$PEFF = P - 5 \quad [1]$$

$$ET = \left(\frac{ab}{c}\right) 10^3 \quad [2]$$

$$a = D - SMD_{t-1} \quad [3]$$

$$b = 0.968e^{(0.0875TMAX+1.5552)-8.3} \quad [4]$$

$$c = 1 + 10.88e^{-0.00173MAR} \quad [5]$$

$$SMD = SMD_{t-1} - PEFF + ET. \quad [6]$$

The KBDI values were converted to KBDI anomalies based on a percentile method. We used Climate Data Operators (1.9.9rc2) to carry out the calculation. First, the 99th KBDI percentile for the 1980 to 2020 time period was estimated relative to the long-term daily minimum (timmin) and maximum (timmax) KBDI using the *timptcl* function. This returns the KBDI value matching the 99th percentile for the daily 41-y time series (1980 to 2020) with values

ranging from 0 to 203 mm. The original daily KBDI values were compared with the 99th percentile values to determine the KBDI anomalies. For example, if the 99th percentile KBDI value was 150 mm (meaning that this value was exceeded only 1% of the time) and if the daily observed KBDI value was 170 mm, then the KBDI percentile anomaly would be 20 mm greater than the 99th percentile value (i.e., the drying was 20 mm greater than three sigma values). Or, if the daily observed KBDI was 100 mm, then the percentile anomaly would be -50 mm, meaning the KBDI is 50 mm lower (wetter) than three sigma. We compared using 95th percentiles and found the threshold value did not alter our conclusions.

Statistical Model. A statistical model was developed (using R version 3.6.0) to predict the number of satellite-derived active fire pixels from the KBDI fire danger index. The model was developed for each state, integrating the number of active fire pixels for the March to August (MAMJJA) period and averaging KBDI for the same period. Active fire data from MODIS Terra and Aqua were used, providing an 18 y (2003 to 2020) time period compared to 9 y for VIIRS. For each state, individual linear models were fit between average MAMJJA KBDI and total MAMJJA fire pixel counts using the years 2003 to 2019 (excluding 2020). The fitted model was used to predict fire activity for 2020 given the 2020 MAMJJA average KBDI. We calculated the difference between the predicted number of MAMJJA active fire pixels and the observed number with the departure in fires due to COVID-19 impacts. The analysis was carried out for all lands and again for just federally owned lands. Combining the data for a single southeastern United States model showed a similar departure in the expected number of active fires from the active fires that were actually documented in 2020 (*SI Appendix, Fig. S9*).

Data Availability. All study data are included in the article and/or *SI Appendix*.

ACKNOWLEDGMENTS. We appreciate the development and maintenance of the NASA FIRMS that distribute NRT active fire data and the NASA GMAO for providing MERRA-2. B.P. acknowledges support from the NASA Carbon Monitoring System and the NASA Rapid Response and Novel Research in Earth Sciences programs. The work is visualized via the NASA COVID-19 Dashboard (<https://earthdata.nasa.gov/covid19>). We thank Alex Varner for his field insights into how COVID-19 affected fire management and thank Joe Noble and Eli Simonson for helping to set up the Tall Timbers active fire tracker (<https://talltimbers.org/nasa-prescribed-fire-covid19/>) and also thank the two anonymous reviewers for their constructive comments.

1. F. Liu *et al.*, Abrupt decline in tropospheric nitrogen dioxide over China after the outbreak of COVID-19. *Sci. Adv.* **6**, eabc2992 (2020).
2. P. P. Patel, S. Mondal, K. G. Ghosh, Some respite for India's dirtiest river? Examining the Yamuna's water quality at Delhi during the COVID-19 lockdown period. *Sci. Total Environ.* **744**, 140851 (2020).
3. T. Lecocq *et al.*, Global quieting of high-frequency seismic noise due to COVID-19 pandemic lockdown measures. *Science* **369**, 1338–1343 (2020).
4. C. Small, D. Sousa, Spatiotemporal evolution of COVID-19 infection and detection within night light networks: Comparative analysis of USA and China. *Appl. Netw. Sci.* **6**, 10 (2021).
5. D. L. Goldberg, *et al.*, Disentangling the impact of the COVID-19 lockdowns on urban NO₂ from natural variability. *Geophys. Res. Lett.* **47**, e2020GL089269 (2020).
6. A. P. Yunus, Y. Masago, Y. Hijioaka, COVID-19 and surface water quality: Improved lake water quality during the lockdown. *Sci. Total Environ.* **731**, 139012 (2020).
7. C. Le Quéré *et al.*, Temporary reduction in daily global CO₂ emissions during the COVID-19 forced confinement. *Nat. Clim. Chang.* **10**, 647–653 (2020).
8. Z. Liu *et al.*, Near-real-time monitoring of global CO₂ emissions reveals the effects of the COVID-19 pandemic. *Nat. Commun.* **11**, 5172 (2020).
9. B. Weir, *et al.*, Regional impacts of COVID-19 on carbon dioxide detected worldwide from space, in press.
10. P. Friedlingstein *et al.*, Global carbon budget 2020. *Earth Syst. Sci. Data* **12**, 3269–3340 (2020).
11. N. S. Diffenbaugh *et al.*, The COVID-19 lockdowns: A window into the Earth System. *Nat. Rev. Earth Environ.* **1**, 470–481 (2020).
12. J. L. Laughner, *et al.*, The 2020 COVID-19 pandemic and atmospheric composition: Back to the future. *Proc. Natl. Acad. Sci. U.S.A.*
13. G. C. Hurtt *et al.*, Harmonization of global land use change and management for the period 850–2100 (LUH2) for CMIP6. *Geosci. Model Dev.* **13**, 5425–5464 (2020).
14. N. Andela *et al.*, A human-driven decline in global burned area. *Science* **356**, 1356–1362 (2017).
15. K. K. McLauchlan *et al.*, Fire as a fundamental ecological process: Research advances and frontiers. *J. Ecol.* **108**, 2047–2069 (2020).
16. D. M. J. S. Bowman *et al.*, Vegetation fires in the Anthropocene. *Nat. Rev. Earth Environ.* **1**, 500–515 (2020).
17. J. K. Balch *et al.*, Human-started wildfires expand the fire niche across the United States. *Proc. Natl. Acad. Sci. U.S.A.* **114**, 2946–2951 (2017).
18. M. A. Melvin, "2020 national prescribed fire use report" (Tech. Bulletin 04-20, Coalition of Prescribed Fire Councils, 2020).
19. K. M. Navarro *et al.*, Wildland firefighter exposure to smoke and COVID-19: A new risk on the fire line. *Sci. Total Environ.* **760**, 144296 (2021).
20. M. P. Thompson, J. Bayham, E. Belval, Potential COVID-19 outbreak in fire camp: Modeling scenarios and interventions. *Fire (Basel)* **3**, 38 (2020).
21. S. Archibald, C. E. R. Lehmann, J. L. Gómez-Dans, R. A. Bradstock, Defining pyromes and global syndromes of fire regimes. *Proc. Natl. Acad. Sci. U.S.A.* **110**, 6442–6447 (2013).
22. J. L. McCarty, C. O. Justice, S. Korontzi, Agricultural burning in the Southeastern United States detected by MODIS. *Remote Sens. Environ.* **108**, 151–162 (2007).
23. L. N. Kobziar, D. Godwin, L. Taylor, A. C. Watts, Perspectives on trends, effectiveness, and impediments to prescribed burning in the Southern U.S. *Forests* **6**, 561–580 (2015).
24. J. M. Johnston *et al.*, Development of the user requirements for the Canadian Wild-FireSat Satellite Mission. *Sensors (Basel)* **20**, 5081 (2020).
25. H. K. Nowell, C. D. Holmes, K. Robertson, C. Teske, J. K. Hiers, A new picture of fire extent, variability, and drought interaction in prescribed fire landscapes: Insights from Florida government records. *Geophys. Res. Lett.* **45**, 7874–7884 (2018).
26. A. M. Chiodi, N. S. Larkin, J. M. Varner, An analysis of Southeastern US prescribed burn weather windows: Seasonal variability and El Niño associations. *Int. J. Wildland Fire* **27**, 176–189 (2018).
27. S. A. Drury, H. M. Rauscher, E. M. Banwell, S. Huang, T. L. Lavezzo, The interagency fuels treatment decision support system: Functionality for fuels treatment planning. *Fire Ecol.* **12**, 103–123 (2016).
28. J. J. Keetch, G. M. Byram, *A Drought Index for Forest Fire Control* (US Department of Agriculture, Forest Service, Southeastern Forest Experiment, 1968).
29. Z. Jiang *et al.*, Unexpected slowdown of US pollutant emission reduction in the past decade. *Proc. Natl. Acad. Sci. U.S.A.* **115**, 5099–5104 (2018).
30. W. E. Cascio, Wildland fire smoke and human health. *Sci. Total Environ.* **624**, 586–595 (2018).
31. L. T. Kelly, L. Brotons, Using fire to promote biodiversity. *Science* **355**, 1264–1265 (2017).
32. S. L. Stephens *et al.*, Fire and climate change: Conserving seasonally dry forests is still possible. *Front. Ecol. Environ.* **18**, 354–360 (2020).
33. J. Pollet, P. N. Omi, Effect of thinning and prescribed burning on crown fire severity in ponderosa pine forests. *Int. J. Wildland Fire* **11**, 1–10 (2002).

34. K. C. Ryan, E. E. Knapp, J. M. Varner, Prescribed fire in North American forests and woodlands: History, current practice, and challenges. *Front. Ecol. Environ.* **11**, e15–e24 (2013).
35. J. S. Glitzenstein, D. R. Streng, R. E. Masters, K. M. Robertson, S. M. Hermann, Fire-frequency effects on vegetation in north Florida pinelands: Another look at the long-term Stoddard Fire Research Plots at Tall Timbers Research Station. *For. Ecol. Manage.* **264**, 197–209 (2012).
36. W. H. McNab, M. B. Edwards Jr., W. A. Hough, Estimating fuel weights in slash pine-palmetto stands. *For. Sci.* **24**, 345–358 (1978).
37. K. M. Robertson, S. M. Hermann, E. L. Staller, Frequent prescribed fire sustains old field Loblolly Pine–Shortleaf Pine Woodland Communities: Results of a 53-year study. *J. For.*, 10.1093/jofore/fvab035 (2021).
38. J. T. Abatzoglou, A. P. Williams, Impact of anthropogenic climate change on wildfire across western US forests. *Proc. Natl. Acad. Sci. U.S.A.* **113**, 11770–11775 (2016).
39. W. M. Jolly *et al.*, Climate-induced variations in global wildfire danger from 1979 to 2013. *Nat. Commun.* **6**, 7537 (2015).
40. J. K. Hiers *et al.*, Prescribed fire science: The case for a refined research agenda. *Fire Ecol.* **16**, 11 (2020).
41. M. Rodrigues, P. J. Gelabert, A. Ameztegui, L. Coll, C. Vega-García, Has COVID-19 halted winter-spring wildfires in the Mediterranean? Insights for wildfire science under a pandemic context. *Sci. Total Environ.* **765**, 142793 (2021).
42. M. Amador-Jiménez, N. Millner, C. Palmer, R. T. Pennington, L. Sileci, The unintended impact of Colombia's covid-19 lockdown on forest fires. *Environ. Resour. Econ.* **76**, 1081–1105 (2020).
43. L. Giglio, J. Desloîtres, C. O. Justice, Y. J. Kaufman, An enhanced contextual fire detection algorithm for MODIS. *Remote Sens. Environ.* **87**, 273–282 (2003).
44. L. Giglio, W. Schroeder, C. O. Justice, The collection 6 MODIS active fire detection algorithm and fire products. *Remote Sens. Environ.* **178**, 31–41 (2016).
45. T. J. Hawbaker, V. C. Radeloff, A. D. Syphard, Z. Zhu, S. I. Stewart, Detection rates of the MODIS active fire product in the United States. *Remote Sens. Environ.* **112**, 2656–2664 (2008).
46. G. R. van der Werf *et al.*, Global fire emissions and the contribution of deforestation, savanna, forest, agricultural, and peat fires (1997–2009). *Atmos. Chem. Phys.* **10**, 11707–11735 (2010).
47. A. Darmonev, A. da Silva, “The Quick Fire Emissions Dataset (QFED): Documentation of versions 2.1, 2.2 and 2.4” (NASA/TM–2013–104606/Vol 32, NASA, 2013).
48. R. Gelaro *et al.*, The modern-era retrospective analysis for research and applications, version 2 (MERRA-2). *J. Clim.* **30**, 5419–5454 (2017).
49. R. H. Reichle *et al.*, Assessment of MERRA-2 land surface hydrology estimates. *J. Clim.* **30**, 2937–2960 (2017).
50. E. K. Brown, J. Wang, Y. Feng, US wildfire potential: A historical view and future projection using high-resolution climate data. *Environ. Res. Lett.* **16**, 034060 (2021).